

# Chasing the two-Higgs-doublet model via electroweak corrections at $e^+e^-$ colliders

Pia Bredt ,<sup>1</sup> Tatsuya Banno ,<sup>2</sup> Marius Höfer ,<sup>3</sup> Syuhei Iguro ,<sup>4, 5</sup>  
Wolfgang Kilian ,<sup>1</sup> Yang Ma ,<sup>6</sup> Jürgen Reuter ,<sup>7</sup> and Hantian Zhang ,<sup>8,\*</sup>

<sup>1</sup>*Center for Particle Physics Siegen, University of Siegen, Walter-Flex-Str. 3, 57072 Siegen, Germany*

<sup>2</sup>*Department of Physics, Nagoya University, Nagoya 464-8602, Japan*

<sup>3</sup>*Institute for Theoretical Physics, Karlsruhe Institute of Technology,  
Wolfgang-Gaede-Str. 1, 76131 Karlsruhe, Germany*

<sup>4</sup>*Institute for Advanced Research, Nagoya University, Nagoya 464-8601, Japan*

<sup>5</sup>*Kobayashi-Maskawa Institute for the Origin of Particles and the Universe, Nagoya University, Nagoya 464-8602, Japan*

<sup>6</sup>*Center for Cosmology, Particle Physics and Phenomenology,*

*Université catholique de Louvain, B-1348 Louvain-la-Neuve, Belgium*

<sup>7</sup>*Deutsches Elektronen-Synchrotron DESY, Notkestr. 85, 22607 Hamburg, Germany*

<sup>8</sup>*Theoretical Physics Department, CERN, 1211 Geneva 23, Switzerland*

We present a comprehensive study of Higgs boson production associated with a neutrino pair at  $e^+e^-$  colliders ( $e^+e^- \rightarrow h\nu\bar{\nu}$ ) at the next-to-leading-order accuracy in both the Standard Model and the two-Higgs-doublet model. We show that new physics effects from the extended Higgs sector can be probed through electroweak corrections, which lead to several percent deviations from the Standard Model predictions in total cross sections and differential distributions, even in the alignment limit. This highlights the potential of precision studies at future  $e^+e^-$  colliders for searching new physics.

The Higgs boson discovered at the Large Hadron Collider (LHC) [1, 2] has completed the particle content predicted by the Standard Model (SM) [3–5]. Despite its great success, fundamental problems such as the origins of baryon asymmetry of the universe and dark matter persist, necessitating new physics beyond the SM (BSM). In this context, precise studies of Higgs boson properties and direct searches of new physics form two complementary focuses in modern particle physics. Over the past decade, the accuracy of Higgs-sector measurements has been greatly improved at the LHC, while there is still room for new physics effects at the ten percent level [6, 7]. Although the LHC is well-suited for studying the gross picture of the Higgs sector, future  $e^+e^-$  colliders such as FCC-ee, CEPC, ILC/LCF and CLIC [8–15] are required for the determination of Higgs boson properties at the electroweak scale with few permille level accuracy.

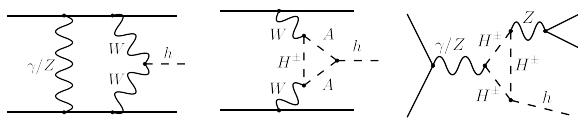
In this paper, we show that there are realistic opportunities for searching new physics through the precision program at future high-energy  $e^+e^-$  colliders, particularly via electroweak (EW) corrections to scattering processes. We demonstrate this possibility through a comprehensive study of single Higgs production ( $e^+e^- \rightarrow h + \nu_\ell \bar{\nu}_\ell$  with  $\ell = e, \mu, \tau$ ) at the next-leading-order (NLO) EW accuracy in both the SM and two-Higgs-doublet model (2HDM). The 2HDM is one of the simplest extensions of the SM and has rich phenomenology [16]. This model can resolve the vacuum meta-stability issue [17] and provide strong first-order electroweak phase transition for baryogenesis [18] and detectable gravitational waves [19]. It often appears as a low-energy scalar sector of more UV-complete theories, for example, the left-right

symmetric models [20–22] and supersymmetric (SUSY) models [23, 24]. In the 2HDM, there exists also an alignment limit where the discovered Higgs boson behaves exactly as the SM one at the tree level. We show that even in this limit, NLO EW corrections involving new particles can induce few percent effects with respect to the SM predictions, thereby offering an important window to access this model.

In the literature, the on-shell Higgsstrahlung process,  $e^+e^- \rightarrow Zh$ , has been intensively investigated. For example, full NLO EW corrections in the 2HDM and SUSY models are computed in Refs. [25–28], and the higher-order calculations in the SM for related triangle and box form factors are computed in Refs. [29–33]. However, the more complicated off-shell single Higgs production  $e^+e^- \rightarrow h\nu\bar{\nu}$  is not so well studied. Pioneering works for this  $2 \rightarrow 3$  process include the full NLO EW corrections in the SM [34–36] and one-loop triangle form factor corrections in the SUSY models [37–40], while a complete NLO EW study in BSM theories is still missing. This process is advantageous, since at higher center-of-mass energies,  $\sqrt{s} = 365$  and  $550$  GeV, its cross section is roughly an order of magnitude larger than those of  $e^+e^- \rightarrow h\ell\bar{\ell}$  processes. In particular, the fact that its cross section at larger  $\sqrt{s}$  is dominated by  $WW$  fusion allows an independent probe of new physics effects other than  $Zh$  production.

We follow the convention of 2HDM in Refs. [41–43]. The two Higgs doublets are denoted by  $\Phi_1$  and  $\Phi_2$ , each acquiring a vacuum expectation value (vev). If both doublets couple to fermions as in the SM, the neutral scalars induce large tree level flavor changing neutral currents (FCNCs) in general. To prevent such large FCNCs, assigning the  $\mathbb{Z}_2$  symmetry charge is helpful [44, 45]. As a result, there are four types of Yukawa structures depending on the  $\mathbb{Z}_2$  charge assignment [46, 47]. The CP-

\* [hantian.zhang@cern.ch](mailto:hantian.zhang@cern.ch)

FIG. 1. Diagrams for  $e^+e^- \rightarrow h\nu\bar{\nu}$  at NLO EW in 2HDM.

conserving Higgs potential is

$$V = m_1^2 \Phi_1^\dagger \Phi_1 + m_2^2 \Phi_2^\dagger \Phi_2 - m_{12}^2 (\Phi_1^\dagger \Phi_2 + \Phi_2^\dagger \Phi_1) + \frac{\lambda_1}{2} (\Phi_1^\dagger \Phi_1)^2 + \frac{\lambda_2}{2} (\Phi_2^\dagger \Phi_2)^2 + \frac{\lambda_3}{2} (\Phi_1^\dagger \Phi_1)(\Phi_2^\dagger \Phi_2) + \frac{\lambda_4}{2} (\Phi_1^\dagger \Phi_2)(\Phi_2^\dagger \Phi_1) + \frac{\lambda_5}{2} [(\Phi_1^\dagger \Phi_2)^2 + (\Phi_2^\dagger \Phi_1)^2], \quad (1)$$

where the  $\mathbb{Z}_2$  symmetry ( $\Phi_1 \rightarrow -\Phi_1$  and  $\Phi_2 \rightarrow \Phi_2$ ) is softly broken by the  $m_{12}^2$  term. After spontaneous symmetry breaking, two mixing angles  $\alpha$  and  $\beta$  can be introduced to obtain the mass eigenstates. In addition to the 125 GeV SM-like Higgs boson  $h$ , we have four scalars: charged scalars  $H^\pm$ , neutral scalar  $H$  and pseudoscalar  $A$ . The parameter  $c_{\beta\alpha} \equiv \cos(\beta - \alpha)$  governs the mixing between CP-even scalars  $h$  and  $H$ , while  $t_\beta \equiv \tan(\beta)$  represents the ratio of two vevs and determines the Yukawa couplings. Note that the so-called Higgs alignment limit is realized in  $c_{\beta\alpha} = 0$  such that the  $h$  is aligned with the SM Higgs. Now the extended Higgs sector is parametrized by  $c_{\beta\alpha}$ ,  $t_\beta$ ,  $\lambda_5$ ,  $m_H$ ,  $m_A$ ,  $m_{H^\pm}$ .

We pursue a complete NLO EW calculation in the 2HDM for  $e^+e^- \rightarrow h\nu\bar{\nu}$  by employing the automated NLO framework [48–52] of the multi-purpose Monte-Carlo generator **Whizard** [53, 54] with an interface to generic one-loop amplitude providers **OpenLoops2** [55] and **Recola** [56, 57] for the SM, and **Recola2** [57] for the 2HDM. We note that **OpenLoops2** supports the 2HDM at NLO QCD [58]. The representative 2HDM Feynman diagrams are shown in Fig. 1. In **Whizard** for this study, a massive electron-positron beam setup is used such that initial state collinear singularities are regulated, while soft singularities are handled in an automated way within the Frixione-Kunszt-Signer subtraction [59]. In the SM case, we compare our NLO EW cross section with Ref. [35] and find agreement at the 0.2% level at  $\sqrt{s} = 500$  GeV. The small residual discrepancy can be attributed to differences in the treatment of complex mass [36, 55, 60] and the structure function approach [61–63]. In the 2HDM case, electroweak renormalization schemes are developed in Refs. [43, 64–66]. We employ two on-shell renormalization schemes defined in Ref. [43]. The default on-shell scheme for mixing angles in **Recola2** serves as our reference scheme, while the background-field approach is used to estimate scheme uncertainties. The  $\lambda_5$  is renormalized in the  $\overline{\text{MS}}$  scheme. We compare our NLO EW cross sections for  $pp \rightarrow h\mu^+\nu_\mu$  in several 2HDM benchmarks with Ref. [43] using **HAWK** [67] and find excellent agreement. This is one of the most extensive NLO applications of **Whizard**, not

	$\sqrt{s} = 365$ GeV		$\sqrt{s} = 550$ GeV	
	LO [fb]	NLO EW [fb]	LO [fb]	NLO EW [fb]
SM	55.79	52.44(1)	97.82(1)	88.45(2)
2HDM	55.71	51.45(1)	97.67(1)	86.59(2)
Rel.Dif.	-0.1%	-1.9%	-0.2%	-2.1%
2HDM (aligned)	55.79	51.58(1)	97.81(1)	86.83(2)
Rel.Dif.	0.0%	-1.7%	0.0%	-1.8%

TABLE I. Total cross sections for  $e^+e^- \rightarrow h\nu\bar{\nu}$  in the SM and the type I 2HDM benchmark without cuts, and the alignment limit is realized with  $\cos(\beta - \alpha) = 0$ . The relative difference  $(\sigma_{2\text{HDM}} - \sigma_{\text{SM}})/\sigma_{\text{SM}}$  is reported at LO and NLO. Monte-Carlo integration errors larger than 0.01 fb are indicated in brackets.

by the complexity of single process but by the massive scan over parameter points performed for the same process as outlined below, capitalizing on the massive parallelization features of **Whizard** [68, 69].

In the following benchmark, we compare predictions between the SM and type I 2HDM. The SM input parameters are  $G_F = 1.166378 \times 10^{-5}$  GeV,  $m_h = 125.2$  GeV,  $m_Z = 91.1539$  GeV,  $\Gamma_Z = 2.4946$  GeV,  $m_W = 80.3407$  GeV,  $\Gamma_W = 2.14$  GeV,  $m_b = 4.183$  GeV,  $m_t = 172.56$  GeV,  $m_e = 5.110 \times 10^{-4}$  GeV, and the  $G_\mu$  scheme is employed. The  $W$  and  $Z$  masses and widths are pole values, which are converted from measured on-shell values. Light quark and lepton mass effects are negligible for this process, except for the electron mass due to large logarithms from the initial-state radiation (ISR). A 2HDM benchmark point allowed by theoretical and experimental constraints based on **HiggsTools** [70] is  $m_H = m_{H^\pm} = 400$  GeV,  $m_A = 435$  GeV,  $c_{\beta\alpha} = 0.03734$ ,  $t_\beta = 1.88$ ,  $\lambda_5 = -2.54$ . The on-shell renormalization scheme for mixing angles is employed, and the renormalization scale for  $\lambda_5$  set to  $\sqrt{s}$ .

In Table I we present the LO and NLO EW total cross sections at  $\sqrt{s} = 365$  and 550 GeV (both unpolarized) in the SM and the 2HDM benchmark, as well as in the alignment limit  $c_{\beta\alpha} = 0$ . At LO, increasing the energy from  $\sqrt{s} = 365$  to 550 GeV enhances the cross section by about 75%, both in the SM and the 2HDM. For both energies, we find only a permille level reduction of the cross section in the 2HDM compared to the SM, which becomes negligible in the alignment limit. The situation changes at NLO: while the EW corrections are negative in all cases, they are more pronounced in the 2HDM, even in the alignment limit. Specifically, the reduction amounts to -6.0% (-9.6%) in the SM at  $\sqrt{s} = 365$  (550) GeV, compared to -7.5% (-11.2%) and -7.6% (-11.3%) in the 2HDM with and without alignment. Therefore, we conclude that NLO EW corrections are a very sensitive probe to BSM effects of our 2HDM benchmarks.

In Fig. 2 we show the differential cross section as a function of the normalized three-momentum of the Higgs,  $\bar{p}_h \equiv |\vec{p}_h|/\sqrt{s}$ , again for two energies  $\sqrt{s} = 365$  and 550 GeV. We focus on the comparison between the SM and 2HDM at NLO. In the upper panel, for  $\sqrt{s} =$

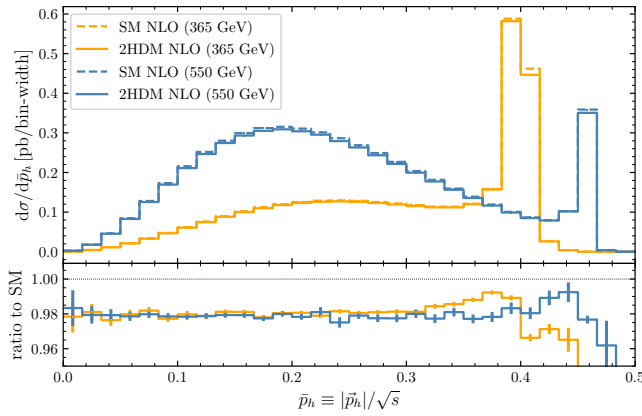


FIG. 2. Top panel: differential cross sections at NLO as a function of the normalised Higgs three-momentum  $\bar{p}_h \equiv |\bar{p}_h|/\sqrt{s}$  at  $\sqrt{s} = 365$  GeV (orange) and  $\sqrt{s} = 550$  GeV (blue), in the SM (dashed) and 2HDM (solid). Bottom panel: ratios of the 2HDM predictions to the SM ones at NLO.

365 (550) GeV the peak corresponding to on-shell  $Zh$  production, with the  $Z$  subsequently decaying into  $\nu\bar{\nu}$ , is located at  $\bar{p}_h \approx 0.401$  ( $\bar{p}_h \approx 0.459$ ), and values up to  $\bar{p}_h \approx 0.441$  ( $\bar{p}_h \approx 0.474$ ) are kinematically allowed. Most of the cross section actually comes from the  $WW$ -fusion contribution at lower values of  $\bar{p}_h$ , which is more spread out and does not lead to a peak like the  $Zh$  channel. We observe that the relative contribution from the  $Zh$  channel decreases when going to higher  $\sqrt{s}$ . In the lower panel we show the ratios of the 2HDM predictions to those in the SM. Both for  $\sqrt{s} = 365$  and 550 GeV we observe that the BSM effects lead to an overall reduction of the cross sections by about 2%, in line with the findings for the total cross sections in Table I. For most of the range of  $\bar{p}_h$  the shift is flat, becoming smaller just below the  $Zh$  peak, but larger once we cross it to larger values of  $\bar{p}_h$ . The separation of  $WW$  and  $Zh$  channels in the differential distribution enables simultaneous probes of 2HDM effects in a single process. This separation could be further facilitated by the use of polarized beams which is beyond the scope of this study.

Moreover, at  $\sqrt{s} = 240$  GeV we find a similar  $-2\%$  relative difference with respect to the SM prediction (43.87 fb) at NLO EW. Nevertheless, since the ISR effect beyond NLO can reach  $\mathcal{O}(10\%)$  at 240 GeV [35], we focus on  $\sqrt{s} = 365$  and 550 GeV, where the higher-order ISR effects are only at the few permille level. We also investigate the  $Zh$ -mediated process  $e^+e^- \rightarrow h\mu^+\mu^-$  and find much smaller cross sections of 4.04 (1.72) fb at  $\sqrt{s} = 365$  (550) GeV. Hence, the process  $e^+e^- \rightarrow h\nu\bar{\nu}$  is advantageous in probing new physics effects due to large  $WW$ -fusion contributions.

We emphasize that this indirect probe at future  $e^+e^-$  colliders is complementary to the direct searches for new physics. At the LHC, single production of an additional scalar via gauge interaction is suppressed by the  $hH$

mixing, whereas production through Yukawa interaction is highly model dependent. Although electroweak pair production of additional scalars, e.g.,  $pp \rightarrow W^+ \rightarrow H^+H$  is not suppressed by the mixing, the production rates decrease rapidly with increasing scalar masses. While at  $e^+e^-$  colliders, if the collision energy is sufficiently high, e.g., in the benchmark with  $\sqrt{s} = 550$  GeV and  $m_H = 400$  GeV, the process  $e^+e^- \rightarrow Z^* \rightarrow ZH$  becomes accessible, but its cross section remains suppressed by the mixing and vanishes in the alignment limit. In contrast, for  $e^+e^- \rightarrow h\nu\bar{\nu}$  we show that the EW corrections can be sizable even in the alignment limit, thereby providing an important complementary window to probe the model.

In the next stage, we present a comprehensive analysis for four types of  $\mathbb{Z}_2$ -symmetric 2HDMs: type I, II, X (lepton specific) and Y (flipped). We generate the parameter set with `ScannerS` [71, 72] and `HiggsTools` [70] based on `HiggsBounds` [73–76] and `HiggsSignals` [77, 78] to take theoretical and experimental constraints into account. For instance, these constraints include tree-level perturbative unitarity, boundedness from below and electroweak vacuum stability as theoretical constraints and electroweak precision observables, flavor-changing processes, direct searches at LHC and LEP. In our set up, the additional scalars are degenerate. The remaining free parameters are  $m_\phi \equiv m_H = m_A = m_{H^\pm}$ ,  $c_{\beta\alpha}$ ,  $t_\beta$  and  $\lambda_5$ , which are chosen from the 95% confidence level (C.L.) allowed region. In total, we generate 30 000 parameter points for the type I, II and Y, and 70 000 parameter points for the type X.

In our sensitivity analysis, the 2HDM predictions in parameter planes of  $c_{\beta\alpha}$ ,  $\lambda_5$ ,  $t_\beta$ ,  $\cos(\alpha)/\sin(\beta)$ ,  $m_\phi$  are presented in Figs. 3 and 4 at  $\sqrt{s} = 365$  GeV, and in Fig. 5 in the appendix for  $\sqrt{s} = 550$  GeV. The relative differences  $(\sigma_{2\text{HDM}} - \sigma_{\text{SM}})/\sigma_{\text{SM}}$  at the LO and NLO are shown for  $|c_{\beta\alpha}| < 0.1$ , covering more than the estimated 95% C.L. allowed range for the least constrained type I 2HDM at future  $e^+e^-$  colliders [79, 80]. To estimate the theoretical uncertainty, we compute the renormalization scheme dependence for mixing angles in the type I 2HDM for hundreds of parameter points, finding the maximal uncertainty of 0.7% (0.8%) for the relative difference at  $\sqrt{s} = 365$  (550) GeV for  $|c_{\beta\alpha}| < 0.1$ . Note that in the difference,  $(\sigma_{2\text{HDM}} - \sigma_{\text{SM}})$ , the missing higher-order SM corrections cancel and do not contribute to the uncertainty. To further reduce the scheme uncertainty, NNLO EW corrections in the 2HDM would be required. On the other hand, the experimental uncertainty of the cross section measurement will reach 0.6% (0.3%) at  $\sqrt{s} = 365$  (500) GeV with  $4.3$  ( $6.4$ )  $\text{ab}^{-1}$  of the data [13]. We expect that the sensitivity difference between  $\sqrt{s} = 500$  and 550 GeV is negligible.

It is shown in Fig. 3 that  $c_{\beta\alpha}$  is the key parameter governing the LO 2HDM deviation from the SM. We first discuss the type I 2HDM plot at  $\sqrt{s} = 365$  GeV. The LO relative difference (red) vanishes as the  $|c_{\beta\alpha}|$  approaches the alignment limit and increases with  $|c_{\beta\alpha}|$  reaching at most  $-1\%$ . At NLO, however, richer phenomena arise

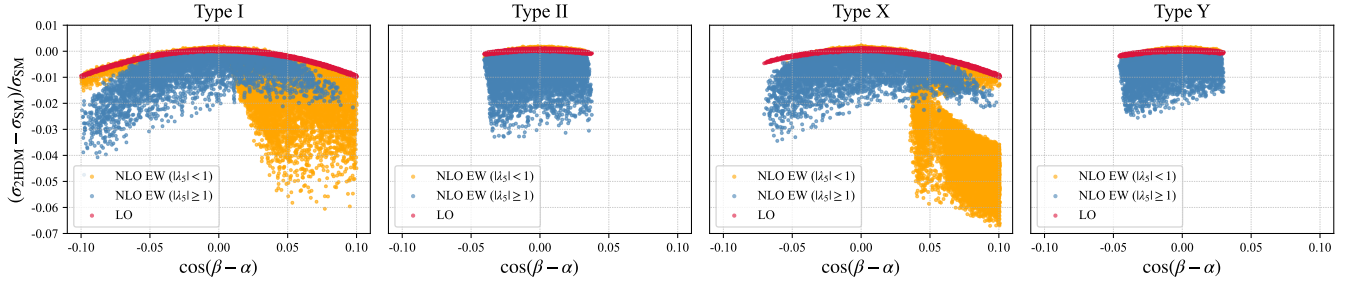


FIG. 3. Type I, II, X and Y 2HDM predictions in the  $\cos(\beta - \alpha)$  plane at  $\sqrt{s} = 365$  GeV within allowed parameter set and  $|\cos(\beta - \alpha)| < 0.1$ . Relative differences with respect to the SM predictions are shown at LO (red) and NLO (orange for  $|\lambda_5| < 1$ , blue for  $|\lambda_5| \geq 1$ ). The combined theoretical and experimental uncertainties are estimated to be 0.92% as explained in the text.

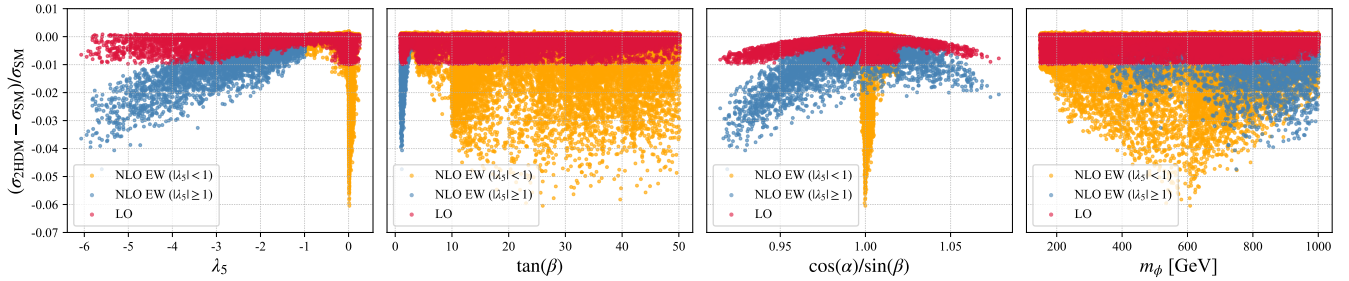


FIG. 4. Type I 2HDM predictions in  $\lambda_5$ ,  $\tan(\beta)$ ,  $\cos(\alpha)/\sin(\beta)$ ,  $m_\phi$  parameter planes at  $\sqrt{s} = 365$  GeV within allowed parameter set and  $|\cos(\beta - \alpha)| < 0.1$ .

that cannot be described by a single parameter. We highlight the impact of EW corrections for the NLO relative difference with two branches separating cases of small  $|\lambda_5| < 1$  (orange) and large  $|\lambda_5| \geq 1$  (blue). The NLO relative difference reaches  $-6\%$  in the small- $|\lambda_5|$  branch and  $-4\%$  in the large- $|\lambda_5|$  branch. The  $-2\%$  deviation in the alignment limit is observed in the large- $|\lambda_5|$  branch, however, it does not imply that this effect is solely driven by the  $\lambda_5$  self-interaction, since Fig. 4 indicates sizable mass effects and top-Yukawa corrections deviating from the SM when  $\cos(\alpha)/\sin(\beta) \neq 1$ . We find that the relative difference at  $\sqrt{s} = 550$  GeV (Fig. 5 in the appendix) is similar to  $\sqrt{s} = 365$  GeV but slightly more pronounced. Since the expected accuracy of the cross section measurement will be better at higher energies, we conclude that the potential 550 GeV operation will be more sensitive to the 2HDM effects. For the remaining plots in Fig. 3, the relative differences reach about  $-7\%$  in the type X, and around  $-3\%$  in the more constrained type II and Y. We note that although our NLO predictions for Higgs production are insensitive to different 2HDM Yukawa structures, the allowed parameter sets across types determine the shapes of distributions, providing restricted ability for the 2HDM-type discrimination. To further distinguish 2HDM types, we need to compute the two-loop EW corrections and/or include Higgs decay channels.

To scrutinize the NLO effects, the relative differences in other parameter planes at  $\sqrt{s} = 365$  GeV are shown

in Fig. 4 for the type I 2HDM. Although the large- $|\lambda_5|$  branch naturally develop sizable effects, the small- $|\lambda_5|$  branch distribution in the  $\cos(\alpha)/\sin(\beta)$  plane is particularly interesting. The ratio  $\cos(\alpha)/\sin(\beta)$  governs the Yukawa coupling between the Higgs and top quark in a same way across all four 2HDM types [81]. The fact that the small- $|\lambda_5|$  branch is localized near  $\lambda_5 \approx 0$  and  $\cos(\alpha)/\sin(\beta) \approx 1$ , yet spread across  $m_\phi$  from 200 GeV to 1 TeV, implies that these large deviations are genuine NLO EW effects, with mixing angles and  $m_\phi$  all playing a role. In addition, there is no clear correlation between the NLO effects and the parameters  $t_\beta$  and  $m_\phi$ . This phenomenon cannot be easily parameterized from an effective field theory approach, highlighting the importance of NLO calculations in UV-complete BSM theories.

In summary, we conduct the first full NLO EW study of Higgs production  $e^+e^- \rightarrow h\nu\bar{\nu}$  in four types of 2HDMs, over vast allowed parameter regions. We find that the 2HDM effects are significantly enhanced at NLO, with deviations from the SM predictions reaching  $-6\%$  to  $-7\%$  with  $|c_{\beta\alpha}| < 0.1$  for  $\sqrt{s} = 365$  and 550 GeV. Even in the alignment limit, these deviations can reach  $-2\%$  to  $-3\%$ , making them experimentally testable. We show that the differential distributions disentangle the  $WW$ -fusion and  $Zh$  channels, allowing simultaneous new physics probes. In a broader context of precision physics at future  $e^+e^-$  colliders, our findings underscore the crucial importance of higher-order electroweak calculations

in UV-complete BSM theories for new physics searches, opening up new windows that are complementary to the LHC searches.

**Acknowledgment:** We thank Georg Weiglein, Johannes Braathen and Jean-Nicolas Lang for useful discussions, and thank Matthias Steinhauser and Gudrun Heinrich for useful comments on the manuscript. H. Zhang is supported by the Swiss National Science Foundation (SNSF) grant TMSGI2 211209, and the Horizon Europe programme under the Marie Skłodowska-Curie Actions (MSCA) grant 101202083 – “HINOVA”. P. Bredt, M. Höfer and W. Kilian are supported by the Deutsche Forschungsgemeinschaft (DFG, German Research Foundation) under grant 396021762 – TRR 257 “Particle

Physics Phenomenology after the Higgs Discovery”. J. Reuter is supported by the DFG under the German Excellence Strategy-EXC 2121 “Quantum Universe”-390833306, and the National Science Centre (Poland) under OPUS research project no. 2021/43/B/ST2/01778. Y. Ma is supported by a Postdoctoral Fellowship of the Fond de la Recherche Scientifique de Belgique (F.R.S.-FNRS), Belgium, and the IISN-FNRS convention 4.4517.08 “Theory of fundamental interactions”. T. Banno is supported by the JST SPRING grant JPMJSP2125. S. Iguro is supported by the JSPS KAKENHI grants 22K21347, 24K22879, 24K23939, 25K17385, JPJSCCA20200002 and the Toyoaki scholarship foundation. S. Iguro and H. Zhang also appreciate the host of Paul Scherrer Institute and University of Zurich, where they stayed during the project.

## Appendix: Supplementary results

In Fig. 5 we show the relative difference in  $\cos(\beta - \alpha)$ ,  $\lambda_5$ ,  $\cos(\alpha)/\sin(\beta)$ ,  $m_\phi$  parameter planes at  $\sqrt{s} = 550$  GeV for the type I 2HDM, respectively. The theoretical uncertainty for the relative differences are estimated to 0.8% for  $|c_{\beta\alpha}| < 0.1$ , and the experimental uncertainty will reach 0.3%. The distributions are similar to the  $\sqrt{s} = 365$  GeV case shown in Figs. 3 and 4, while the relative differences are slightly pronounced at  $\sqrt{s} = 550$  GeV. Given that the expected experimental measurement will be better at 550 GeV, the potential 2HDM searches at this energy will be more advantageous.

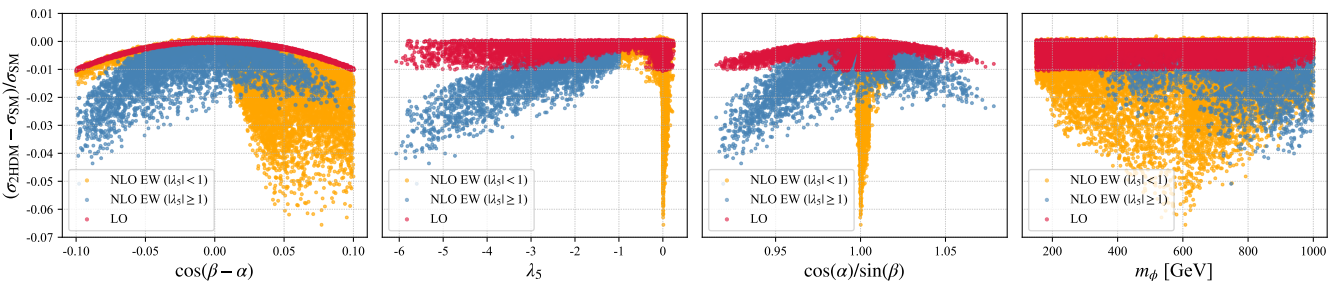


FIG. 5. Type I 2HDM predictions in  $\cos(\beta - \alpha)$ ,  $\lambda_5$ ,  $\cos(\alpha)/\sin(\beta)$ ,  $m_\phi$  parameter planes at  $\sqrt{s} = 550$  GeV within allowed parameter set and  $|\cos(\beta - \alpha)| < 0.1$ . The combined theoretical and experimental uncertainties are estimated to be 0.85% as explained in the main text.

---

[1] ATLAS Collaboration, G. Aad *et al.*, “Observation of a new particle in the search for the Standard Model Higgs boson with the ATLAS detector at the LHC,” *Phys. Lett. B* **716** (2012) 1–29, [arXiv:1207.7214 \[hep-ex\]](https://arxiv.org/abs/1207.7214).

[2] CMS Collaboration, S. Chatrchyan *et al.*, “Observation of a New Boson at a Mass of 125 GeV with the CMS Experiment at the LHC,” *Phys. Lett. B* **716** (2012) 30–61, [arXiv:1207.7235 \[hep-ex\]](https://arxiv.org/abs/1207.7235).

[3] S. L. Glashow, “Partial Symmetries of Weak Interactions,” *Nucl. Phys.* **22** (1961) 579–588.

[4] S. Weinberg, “A Model of Leptons,” *Phys. Rev. Lett.* **19** (1967) 1264–1266.

[5] A. Salam, “Weak and Electromagnetic Interactions,” *Conf. Proc. C* **680519** (1968) 367–377.

[6] CMS Collaboration, A. Tumasyan *et al.*, “A portrait of the Higgs boson by the CMS experiment ten years after the discovery.,” *Nature* **607** no. 7917, (2022) 60–68, [arXiv:2207.00043 \[hep-ex\]](https://arxiv.org/abs/2207.00043). [Erratum: *Nature* 623,

(2023)].

[7] **ATLAS** Collaboration, G. Aad *et al.*, “A detailed map of Higgs boson interactions by the ATLAS experiment ten years after the discovery,” *Nature* **607** no. 7917, (2022) 52–59, [arXiv:2207.00092 \[hep-ex\]](https://arxiv.org/abs/2207.00092). [Erratum: *Nature* 612, E24 (2022)].

[8] **FCC** Collaboration, A. Abada *et al.*, “FCC Physics Opportunities: Future Circular Collider Conceptual Design Report Volume 1,” *Eur. Phys. J. C* **79** no. 6, (2019) 474.

[9] **FCC** Collaboration, M. Benedikt *et al.*, “Future Circular Collider Feasibility Study Report: Volume 1, Physics, Experiments, Detectors,” [arXiv:2505.00272 \[hep-ex\]](https://arxiv.org/abs/2505.00272).

[10] **CEPC Study Group** Collaboration, M. Dong *et al.*, “CEPC Conceptual Design Report: Volume 2 - Physics & Detector,” [arXiv:1811.10545 \[hep-ex\]](https://arxiv.org/abs/1811.10545).

[11] **CEPC Study Group** Collaboration, W. Abdallah *et al.*, “CEPC Technical Design Report: Accelerator,” *Radiat. Detect. Technol. Methods* **8** no. 1, (2024) 1–1105, [arXiv:2312.14363 \[physics.acc-ph\]](https://arxiv.org/abs/2312.14363). [Erratum: *Radiat.Detect.Technol.Methods* 9, 184–192 (2025)].

[12] **ILC International Development Team** Collaboration, A. Aryshev *et al.*, “The International Linear Collider: Report to Snowmass 2021,” [arXiv:2203.07622 \[physics.acc-ph\]](https://arxiv.org/abs/2203.07622).

[13] **Linear Collider Vision** Collaboration, D. Attié *et al.*, “A Linear Collider Vision for the Future of Particle Physics,” [arXiv:2503.19983 \[hep-ex\]](https://arxiv.org/abs/2503.19983).

[14] “Physics and Detectors at CLIC: CLIC Conceptual Design Report,” [arXiv:1202.5940 \[physics.ins-det\]](https://arxiv.org/abs/1202.5940).

[15] E. Adli *et al.*, “The Compact Linear  $e^+e^-$  Collider (CLIC),” [arXiv:2503.24168 \[physics.acc-ph\]](https://arxiv.org/abs/2503.24168).

[16] T. D. Lee, “A Theory of Spontaneous T Violation,” *Phys. Rev. D* **8** (1973) 1226–1239.

[17] M. Sher, “Electroweak Higgs Potentials and Vacuum Stability,” *Phys. Rept.* **179** (1989) 273–418.

[18] A. G. Cohen, D. B. Kaplan, and A. E. Nelson, “Progress in electroweak baryogenesis,” *Ann. Rev. Nucl. Part. Sci.* **43** (1993) 27–70, [arXiv:hep-ph/9302210](https://arxiv.org/abs/hep-ph/9302210).

[19] G. C. Dorsch, S. J. Huber, T. Konstandin, and J. M. No, “A Second Higgs Doublet in the Early Universe: Baryogenesis and Gravitational Waves,” *JCAP* **05** (2017) 052, [arXiv:1611.05874 \[hep-ph\]](https://arxiv.org/abs/1611.05874).

[20] J. C. Pati and A. Salam, “Lepton Number as the Fourth Color,” *Phys. Rev. D* **10** (1974) 275–289. [Erratum: *Phys. Rev. D* 11, 703–703 (1975)].

[21] R. N. Mohapatra and J. C. Pati, “Left-Right Gauge Symmetry and an Isoconjugate Model of CP Violation,” *Phys. Rev. D* **11** (1975) 566–571.

[22] G. Senjanovic and R. N. Mohapatra, “Exact Left-Right Symmetry and Spontaneous Violation of Parity,” *Phys. Rev. D* **12** (1975) 1502.

[23] P. Fayet, “Spontaneously Broken Supersymmetric Theories of Weak, Electromagnetic and Strong Interactions,” *Phys. Lett. B* **69** (1977) 489.

[24] S. P. Martin, “A Supersymmetry primer,” *Adv. Ser. Direct. High Energy Phys.* **18** (1998) 1–98, [arXiv:hep-ph/9709356](https://arxiv.org/abs/hep-ph/9709356).

[25] W. Xie, R. Benbrik, A. Habjia, S. Taj, B. Gong, and Q.-S. Yan, “Signature of 2HDM at Higgs Factories,” *Phys. Rev. D* **103** no. 9, (2021) 095030, [arXiv:1812.02597 \[hep-ph\]](https://arxiv.org/abs/1812.02597).

[26] M. Aiko, S. Kanemura, and K. Mawatari, “Next-to-leading-order corrections to the Higgs strahlung process from electron–positron collisions in extended Higgs models,” *Eur. Phys. J. C* **81** no. 11, (2021) 1000, [arXiv:2109.02884 \[hep-ph\]](https://arxiv.org/abs/2109.02884).

[27] Anisha, F. Arco, S. Di Noi, C. Englert, and M. Mühlleitner, “Z and Higgs Factory Implications of Two Higgs Doublets with First-Order Phase Transitions,” [arXiv:2506.18555 \[hep-ph\]](https://arxiv.org/abs/2506.18555).

[28] S. Heinemeyer, S. Paßehr, and C. Schappacher, “Light Neutral Higgs-Boson Production at  $e^+e^-$  Colliders in the Complex MSSM and NMSSM: A Full One-Loop Analysis,” [arXiv:2507.00931 \[hep-ph\]](https://arxiv.org/abs/2507.00931).

[29] B. A. Kniehl and M. Steinhauser, “Three loop  $O(\alpha_s^2 G_F M_t^2)$  corrections to Higgs production and decay at  $e^+e^-$  colliders,” *Nucl. Phys. B* **454** (1995) 485–505, [arXiv:hep-ph/9508241](https://arxiv.org/abs/hep-ph/9508241).

[30] Y. Gong, Z. Li, X. Xu, L. L. Yang, and X. Zhao, “Mixed QCD-EW corrections for Higgs boson production at  $e^+e^-$  colliders,” *Phys. Rev. D* **95** no. 9, (2017) 093003, [arXiv:1609.03955 \[hep-ph\]](https://arxiv.org/abs/1609.03955).

[31] Q.-F. Sun, F. Feng, Y. Jia, and W.-L. Sang, “Mixed electroweak-QCD corrections to  $e^+e^- \rightarrow HZ$  at Higgs factories,” *Phys. Rev. D* **96** no. 5, (2017) 051301, [arXiv:1609.03995 \[hep-ph\]](https://arxiv.org/abs/1609.03995).

[32] C. Ma, Y. Wang, X. Xu, L. L. Yang, and B. Zhou, “Mixed QCD-EW corrections for Higgs leptonic decay via  $HW^+W^-$  vertex,” *JHEP* **09** (2021) 114, [arXiv:2105.06316 \[hep-ph\]](https://arxiv.org/abs/2105.06316).

[33] A. Freitas and Q. Song, “Two-Loop Electroweak Corrections with Fermion Loops to  $e^+e^- \rightarrow ZH$ ,” *Phys. Rev. Lett.* **130** no. 3, (2023) 031801, [arXiv:2209.07612 \[hep-ph\]](https://arxiv.org/abs/2209.07612).

[34] G. Belanger, F. Boudjema, J. Fujimoto, T. Ishikawa, T. Kaneko, K. Kato, and Y. Shimizu, “Full one loop electroweak radiative corrections to single Higgs production in  $e^+e^-$ ,” *Phys. Lett. B* **559** (2003) 252–262, [arXiv:hep-ph/0212261](https://arxiv.org/abs/hep-ph/0212261).

[35] A. Denner, S. Dittmaier, M. Roth, and M. M. Weber, “Electroweak radiative corrections to single Higgs boson production in  $e^+e^-$  annihilation,” *Phys. Lett. B* **560** (2003) 196–203, [arXiv:hep-ph/0301189](https://arxiv.org/abs/hep-ph/0301189).

[36] A. Denner, S. Dittmaier, M. Roth, and M. M. Weber, “Electroweak radiative corrections to  $e^+e^- \rightarrow \nu\bar{\nu}$  anti- $\nu\bar{\nu}$  H,” *Nucl. Phys. B* **660** (2003) 289–321, [arXiv:hep-ph/0302198](https://arxiv.org/abs/hep-ph/0302198).

[37] H. Eberl, W. Majerotto, and V. C. Spanos, “Radiative corrections to single Higgs boson production in  $e^+e^-$  annihilation,” *Phys. Lett. B* **538** (2002) 353–358, [arXiv:hep-ph/0204280](https://arxiv.org/abs/hep-ph/0204280).

[38] H. Eberl, W. Majerotto, and V. C. Spanos, “Single Higgs boson production at future linear colliders including radiative corrections,” *Nucl. Phys. B* **657** (2003) 378–396, [arXiv:hep-ph/0210038](https://arxiv.org/abs/hep-ph/0210038).

[39] T. Hahn, S. Heinemeyer, and G. Weiglein, “MSSM Higgs boson production at the linear collider: Dominant corrections to the WW fusion channel,” *Nucl. Phys. B* **652** (2003) 229–258, [arXiv:hep-ph/0211204](https://arxiv.org/abs/hep-ph/0211204).

[40] F. Wang, W. Wang, F.-q. Xu, J. M. Yang, and H. Zhang, “Virtual Effects of Split SUSY in Higgs Productions at Linear Colliders,” *Eur. Phys. J. C* **51** (2007) 713–719, [arXiv:hep-ph/0612273](https://arxiv.org/abs/hep-ph/0612273).

[41] M. Aoki, S. Kanemura, K. Tsumura, and K. Yagyu, “Models of Yukawa interaction in the two Higgs doublet

model, and their collider phenomenology,” *Phys. Rev. D* **80** (2009) 015017, [arXiv:0902.4665 \[hep-ph\]](https://arxiv.org/abs/0902.4665).

[42] A. Denner, J.-N. Lang, and S. Uccirati, “NLO electroweak corrections in extended Higgs Sectors with RECOLA2,” *JHEP* **07** (2017) 087, [arXiv:1705.06053 \[hep-ph\]](https://arxiv.org/abs/1705.06053).

[43] A. Denner, S. Dittmaier, and J.-N. Lang, “Renormalization of mixing angles,” *JHEP* **11** (2018) 104, [arXiv:1808.03466 \[hep-ph\]](https://arxiv.org/abs/1808.03466).

[44] E. A. Paschos, “Diagonal Neutral Currents,” *Phys. Rev. D* **15** (1977) 1966.

[45] S. L. Glashow and S. Weinberg, “Natural Conservation Laws for Neutral Currents,” *Phys. Rev. D* **15** (1977) 1958.

[46] V. D. Barger, J. L. Hewett, and R. J. N. Phillips, “New Constraints on the Charged Higgs Sector in Two Higgs Doublet Models,” *Phys. Rev. D* **41** (1990) 3421–3441.

[47] Y. Grossman, “Phenomenology of models with more than two Higgs doublets,” *Nucl. Phys. B* **426** (1994) 355–384, [arXiv:hep-ph/9401311](https://arxiv.org/abs/hep-ph/9401311).

[48] P. M. Bredt, W. Kilian, J. Reuter, and P. Stienemeier, “NLO electroweak corrections to multi-boson processes at a muon collider,” *JHEP* **12** (2022) 138, [arXiv:2208.09438 \[hep-ph\]](https://arxiv.org/abs/2208.09438).

[49] F. Bach, B. C. Nejad, A. Hoang, W. Kilian, J. Reuter, M. Stahlhofen, T. Teubner, and C. Weiss, “Fully-differential Top-Pair Production at a Lepton Collider: From Threshold to Continuum,” *JHEP* **03** (2018) 184, [arXiv:1712.02220 \[hep-ph\]](https://arxiv.org/abs/1712.02220).

[50] B. Chokoufé Nejad, W. Kilian, J. M. Lindert, S. Pozzorini, J. Reuter, and C. Weiss, “NLO QCD predictions for off-shell  $t\bar{t}$  and  $t\bar{t}H$  production and decay at a linear collider,” *JHEP* **12** (2016) 075, [arXiv:1609.03390 \[hep-ph\]](https://arxiv.org/abs/1609.03390).

[51] J. Kalinowski, W. Kilian, J. Reuter, T. Robens, and K. Rolbiecki, “Pinning Down the Invisible Sneutrino at the ILC,” in *International Linear Collider Workshop (LCWS08 and ILC08)*. 1, 2009. [arXiv:0901.4700 \[hep-ph\]](https://arxiv.org/abs/0901.4700).

[52] T. Robens, J. Kalinowski, K. Rolbiecki, W. Kilian, and J. Reuter, “(N)LO Simulation of Chargino Production and Decay,” *Acta Phys. Polon. B* **39** (2008) 1705–1714, [arXiv:0803.4161 \[hep-ph\]](https://arxiv.org/abs/0803.4161).

[53] W. Kilian, T. Ohl, and J. Reuter, “WHIZARD: Simulating Multi-Particle Processes at LHC and ILC,” *Eur. Phys. J. C* **71** (2011) 1742, [arXiv:0708.4233 \[hep-ph\]](https://arxiv.org/abs/0708.4233).

[54] M. Moretti, T. Ohl, and J. Reuter, “O’Mega: An Optimizing matrix element generator,” [arXiv:hep-ph/0102195](https://arxiv.org/abs/hep-ph/0102195).

[55] F. Buccioni, J.-N. Lang, J. M. Lindert, P. Maierhöfer, S. Pozzorini, H. Zhang, and M. F. Zoller, “OpenLoops 2,” *Eur. Phys. J. C* **79** no. 10, (2019) 866, [arXiv:1907.13071 \[hep-ph\]](https://arxiv.org/abs/1907.13071).

[56] S. Actis, A. Denner, L. Hofer, J.-N. Lang, A. Scharf, and S. Uccirati, “RECOLA: RECURsive Computation of One-Loop Amplitudes,” *Comput. Phys. Commun.* **214** (2017) 140–173, [arXiv:1605.01090 \[hep-ph\]](https://arxiv.org/abs/1605.01090).

[57] A. Denner, J.-N. Lang, and S. Uccirati, “Recola2: RECURsive Computation of One-Loop Amplitudes 2,” *Comput. Phys. Commun.* **224** (2018) 346–361, [arXiv:1711.07388 \[hep-ph\]](https://arxiv.org/abs/1711.07388).

[58] S. Iguro, T. Kitahara, Y. Omura, and H. Zhang, “Chasing the two-Higgs doublet model in the di-Higgs boson production,” *Phys. Rev. D* **107** no. 7, (2023) 075017, [arXiv:2211.00011 \[hep-ph\]](https://arxiv.org/abs/2211.00011).

[59] S. Frixione, Z. Kunszt, and A. Signer, “Three jet cross-sections to next-to-leading order,” *Nucl. Phys. B* **467** (1996) 399–442, [arXiv:hep-ph/9512328](https://arxiv.org/abs/hep-ph/9512328).

[60] A. Denner, S. Dittmaier, M. Roth, and L. H. Wieders, “Electroweak corrections to charged-current  $e+e-\rightarrow 4$  fermion processes: Technical details and further results,” *Nucl. Phys. B* **724** (2005) 247–294, [arXiv:hep-ph/0505042](https://arxiv.org/abs/hep-ph/0505042). [Erratum: Nucl.Phys.B 854, 504–507 (2012)].

[61] M. Cacciari, A. Deandrea, G. Montagna, and O. Nicrosini, “QED structure functions: A Systematic approach,” *EPL* **17** (1992) 123–128.

[62] M. Skrzypek and S. Jadach, “Exact and approximate solutions for the electron nonsinglet structure function in QED,” *Z. Phys. C* **49** (1991) 577–584.

[63] M. Skrzypek, “Leading logarithmic calculations of QED corrections at LEP,” *Acta Phys. Polon. B* **23** (1992) 135–172.

[64] S. Kanemura, Y. Okada, E. Senaha, and C. P. Yuan, “Higgs coupling constants as a probe of new physics,” *Phys. Rev. D* **70** (2004) 115002, [arXiv:hep-ph/0408364](https://arxiv.org/abs/hep-ph/0408364).

[65] M. Krause, R. Lorenz, M. Mühlleitner, R. Santos, and H. Ziesche, “Gauge-independent Renormalization of the 2-Higgs-Doublet Model,” *JHEP* **09** (2016) 143, [arXiv:1605.04853 \[hep-ph\]](https://arxiv.org/abs/1605.04853).

[66] L. Altenkamp, S. Dittmaier, and H. Rzehak, “Renormalization schemes for the Two-Higgs-Doublet Model and applications to  $h\rightarrow WW/ZZ\rightarrow 4$  fermions,” *JHEP* **09** (2017) 134, [arXiv:1704.02645 \[hep-ph\]](https://arxiv.org/abs/1704.02645).

[67] A. Denner, S. Dittmaier, S. Kallweit, and A. Mück, “HAWK 2.0: A Monte Carlo program for Higgs production in vector-boson fusion and Higgs strahlung at hadron colliders,” *Comput. Phys. Commun.* **195** (2015) 161–171, [arXiv:1412.5390 \[hep-ph\]](https://arxiv.org/abs/1412.5390).

[68] S. Brass, W. Kilian, and J. Reuter, “Parallel Adaptive Monte Carlo Integration with the Event Generator WHIZARD,” *Eur. Phys. J. C* **79** no. 4, (2019) 344, [arXiv:1811.09711 \[hep-ph\]](https://arxiv.org/abs/1811.09711).

[69] B. Chokoufé Nejad, T. Ohl, and J. Reuter, “Simple, parallel virtual machines for extreme computations,” *Comput. Phys. Commun.* **196** (2015) 58–69, [arXiv:1411.3834 \[physics.comp-ph\]](https://arxiv.org/abs/1411.3834).

[70] H. Bahl, T. Biekötter, S. Heinemeyer, C. Li, S. Paasch, G. Weiglein, and J. Wittbrodt, “HiggsTools: BSM scalar phenomenology with new versions of HiggsBounds and HiggsSignals,” *Comput. Phys. Commun.* **291** (2023) 108803, [arXiv:2210.09332 \[hep-ph\]](https://arxiv.org/abs/2210.09332).

[71] R. Coimbra, M. O. P. Sampaio, and R. Santos, “ScannerS: Constraining the phase diagram of a complex scalar singlet at the LHC,” *Eur. Phys. J. C* **73** (2013) 2428, [arXiv:1301.2599 \[hep-ph\]](https://arxiv.org/abs/1301.2599).

[72] M. Mühlleitner, M. O. P. Sampaio, R. Santos, and J. Wittbrodt, “ScannerS: parameter scans in extended scalar sectors,” *Eur. Phys. J. C* **82** no. 3, (2022) 198, [arXiv:2007.02985 \[hep-ph\]](https://arxiv.org/abs/2007.02985).

[73] P. Bechtle, O. Brein, S. Heinemeyer, G. Weiglein, and K. E. Williams, “HiggsBounds: Confronting Arbitrary Higgs Sectors with Exclusion Bounds from LEP and the Tevatron,” *Comput. Phys. Commun.* **181** (2010) 138–167, [arXiv:0811.4169 \[hep-ph\]](https://arxiv.org/abs/0811.4169).

[74] P. Bechtle, O. Brein, S. Heinemeyer, G. Weiglein, and

K. E. Williams, “HiggsBounds 2.0.0: Confronting Neutral and Charged Higgs Sector Predictions with Exclusion Bounds from LEP and the Tevatron,” *Comput. Phys. Commun.* **182** (2011) 2605–2631, [arXiv:1102.1898 \[hep-ph\]](https://arxiv.org/abs/1102.1898).

[75] P. Bechtle, O. Brein, S. Heinemeyer, O. Stål, T. Stefaniak, G. Weiglein, and K. E. Williams, “HiggsBounds – 4: Improved Tests of Extended Higgs Sectors against Exclusion Bounds from LEP, the Tevatron and the LHC,” *Eur. Phys. J. C* **74** no. 3, (2014) 2693, [arXiv:1311.0055 \[hep-ph\]](https://arxiv.org/abs/1311.0055).

[76] P. Bechtle, D. Dercks, S. Heinemeyer, T. Klingl, T. Stefaniak, G. Weiglein, and J. Wittbrodt, “HiggsBounds-5: Testing Higgs Sectors in the LHC 13 TeV Era,” *Eur. Phys. J. C* **80** no. 12, (2020) 1211, [arXiv:2006.06007 \[hep-ph\]](https://arxiv.org/abs/2006.06007).

[77] P. Bechtle, S. Heinemeyer, O. Stål, T. Stefaniak, and G. Weiglein, “*HiggsSignals*: Confronting arbitrary Higgs sectors with measurements at the Tevatron and the LHC,” *Eur. Phys. J. C* **74** no. 2, (2014) 2711, [arXiv:1305.1933 \[hep-ph\]](https://arxiv.org/abs/1305.1933).

[78] P. Bechtle, S. Heinemeyer, T. Klingl, T. Stefaniak, G. Weiglein, and J. Wittbrodt, “HiggsSignals-2: Probing new physics with precision Higgs measurements in the LHC 13 TeV era,” *Eur. Phys. J. C* **81** no. 2, (2021) 145, [arXiv:2012.09197 \[hep-ph\]](https://arxiv.org/abs/2012.09197).

[79] J. Gu, H. Li, Z. Liu, S. Su, and W. Su, “Learning from Higgs Physics at Future Higgs Factories,” *JHEP* **12** (2017) 153, [arXiv:1709.06103 \[hep-ph\]](https://arxiv.org/abs/1709.06103).

[80] N. Chen, T. Han, S. Li, S. Su, W. Su, and Y. Wu, “Type-I 2HDM under the Higgs and Electroweak Precision Measurements,” *JHEP* **08** (2020) 131, [arXiv:1912.01431 \[hep-ph\]](https://arxiv.org/abs/1912.01431).

[81] G. C. Branco, P. M. Ferreira, L. Lavoura, M. N. Rebelo, M. Sher, and J. P. Silva, “Theory and phenomenology of two-Higgs-doublet models,” *Phys. Rept.* **516** (2012) 1–102, [arXiv:1106.0034 \[hep-ph\]](https://arxiv.org/abs/1106.0034).